Mode dynamics in the amplification of a CW single-frequency laser seed in a multimode fiber taper

Alexei G. Kuznetsov[a], Mikhail D. Gervaziev[a,b], Alexander A. Revyakin[a,b], Mikhail I. Skvortsov[a], Alexandr A. Vlasov[a], Denis S. Kharenko[a,b], Stefan Wabnitz[b,c], and Sergey Babin[a,b]

[a]Institute of Automation and Electrometry SB RAS, Novosibirsk, Russia
[b]Novosibirsk State University, Russia
[c]DIET, Sapienza University of Rome, Italy

ABSTRACT

Spatial beam self-cleaning is one of the most intriguing nonlinear effects in multimode optical fibers: it involves the transformation of a speckled intensity pattern into a smooth beam with a bell-shaped profile at the fiber output. This effect was initially observed above some threshold value of peak power for sub-nanosecond pulses in passive multimode (MM) fibers with graded-index (GRIN) profile; a similar behavior is also observed with other types of fibers or with femtosecond pulse durations. For example, it was reported that a highly-multimode pulsed beam propagating in active (Yb-doped) MM GRIN fiber tapers experiences self-cleaning after amplification to peak powers of ∼20 kW, with a beam quality parameter improved from ∼10 to ∼4. Here we study the amplification of a continuous-wave (CW) single-frequency radiation in a similar MM GRIN fiber taper. Surprisingly, the beam cleaning is observed at much lower output powers. The beam quality is improved to near-Gaussian (<1.5) after amplification to ∼20 W of CW power. We study the dynamics of the output transverse modes by a real-time mode decomposition technique. This reveals a relatively slow (1 Hz range) and unusual evolution in the first few seconds, followed by a relaxation into a stationary state, consisting of a bright spot on a low-power speckled pedestal.

Keywords: Single-frequency Lasers, Fiber Lasers, Fiber Amplifiers, Fibers Tapers, Mode Decomposition, Mode Dynamics

1. INTRODUCTION

It is well-known that singlemode optical fibers provide the main channel of information transmission in optical communications, and are a key component in other real-life applications of fiber optics, such as fiber lasers and fiber sensors. However, MM optical fibers have attracted a lot of interest over the past decade. This is due to the great potential of MM fibers for next-generation telecom systems using spatial-division multiplexing,[1] as well as for the host of nonlinear optical phenomena which are associated with the use of high-energy pulsed multimode laser beams.[2,3] Spatial self-cleaning is one of the most intriguing nonlinear effects in MM fibers, involving the power-induced transformation of a speckled beam into a smooth beam with a bell-shaped profile at the MM fiber output. This effect is observed above some threshold value of peak power for sub-nanosecond pulses.[4] The beam self-cleaning effect is most frequently reported in passive MM fibers with a graded-index (GRIN) profile, but MM beams in other types of fibers may exhibit a similar behavior. For example, in active (Yb-doped) multimode GRIN fiber tapers, a highly-multimode pulsed output beam which generates speckles at low powers, may experience self-cleaning after amplification to peak powers of ∼20 kW, with a beam quality parameter improved from M^2∼10 to M^2∼4.[5,6] More specifically, in Ref.[6] the input laser beam at 1064 nm was injected for propagation from the small to the large core side of the taper, with diode laser pumping in a counter-directional configuration. In this scheme, spatial beam self-cleaning was observed, without any accompanying self-phase modulation induced spectral broadening or frequency conversion. This constitutes a remarkable property of nonlinear MM propagation of sub-nanosecond pulses in MM tapers.

Further author information: (Send correspondence to S.A.B.)
E-mail: babin@iae.nsk.su

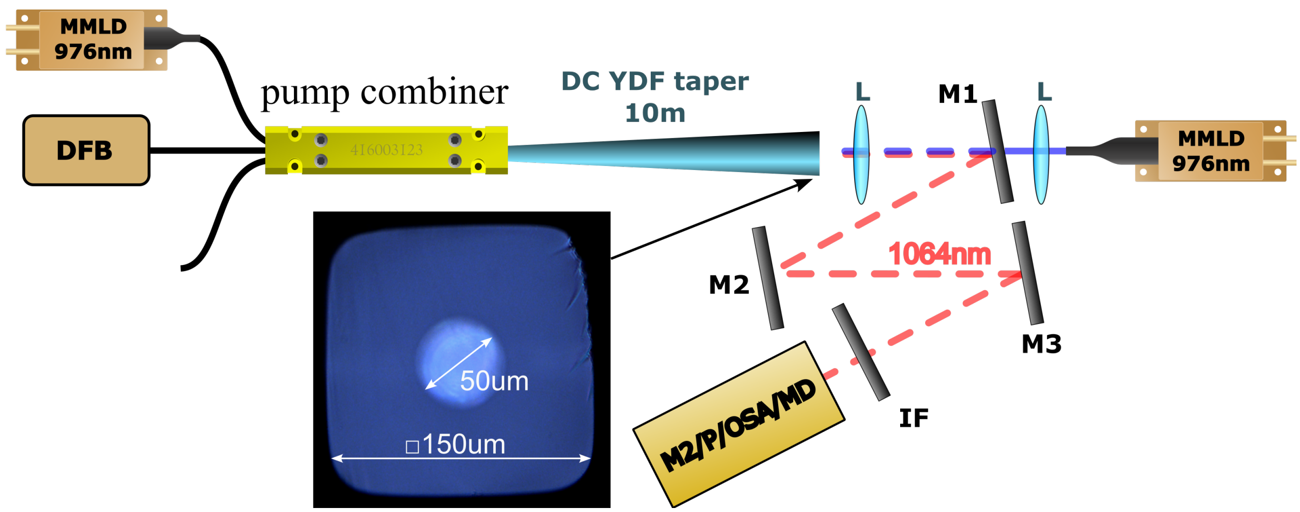

Figure 1. Experimental setup: DFB — single-frequency fiber laser; MM LD — multimode laser diodes at 976 nm; DC YDF — double-clad Yb-doped fiber taper; L –collimating lenses; M1-M3 — dichroic mirrors; IF – interference filter; P/OSA/M^2/MD — characterization setup consisting of power meter, optical spectrum analyzer, beam quality analyzer and mode decomposition setup. Inset: microscopic image of the DC YDF output endface.

Here we study the amplification of a continuous-wave (CW) single-frequency (SF) radiation in a similar type if multimode GRIN fiber taper, and observe a spatial beam cleaning effect at comparatively much lower output powers, with a beam quality improvement to near-Gaussian diffraction-limited beam ($M^2 < 1.5$). We apply both co- and counter-directional pumping, and characterize the output beam in terms of output power, optical and radio-frequency spectrum, heterodyne-measured linewidth, and beam quality factor power dependence. We also perform a detailed analysis of the MM beam spatial properties by a mode decomposition (MD) technique operating in real-time.

2. EXPERIMENTAL SETUP

Our experiment consisted in the amplification of SF radiation from a distributed-feedback (DFB) fiber laser in a MM Yb-doped GRIN fiber taper. The DFB laser was implemented in a polarization-maintaining singlemode fiber; its maximum output power was 15 mW at the wavelength of 1064 nm. The output of this laser seed was coupled to the narrow end of a tapered MM amplifier via $(2 + 1) \times 1$ pump combiner (see Fig. 1). The tapered fiber was a 10 m long double-clad waveguide with a square cladding and a MM GRIN circular core. The rib length in the cross section of the narrow end is 100 µm, the core diameter was ∼33 µm, while at the wide end these values increase to 150 µm and 50 µm, respectively (see the image in Fig. 1). The amplifier was pumped from both ends by two MM laser diodes with a wavelength of 976 nm and an output fiber of 105/125 µm (NA=0.22) through a pump combiner or collimating lenses L, respectively. The output end of the amplifier was cleaved at an angle of ∼10°to reduce Fresnel back reflection. The amplified beam was characterized with the use of dichroic mirrors M1–3 and interference filter (IF).

3. RESULTS AND DISCUSSIONS

The obtained output power of the amplified signal reaches 20.2 W in the presence of 50 W backward pumping and 15 W forward pumping. The measured profile of the output beam has a bright central spot and a weaker halo, repeating the cross-section of the core, with the relative intensities depending on power, see the left inset in Fig. 2(a). The corresponding beam quality parameter M^2 was calculated from the beam divergence (measured at the intensity level of $1/e^2$). In our measurements, we first increased the backward LD pump power from the wide end (output signal 0–15 W with pumping 0–50 W), and then added forward LD pumping from the narrow end (output signal 15–20 W with additional pumping 0–15 W). In this configuration, backward pumping improves the beam quality from ∼10 to ∼4, whereas adding forward pumping leads to a further beam cleaning down to $M^2 < 1.5$.

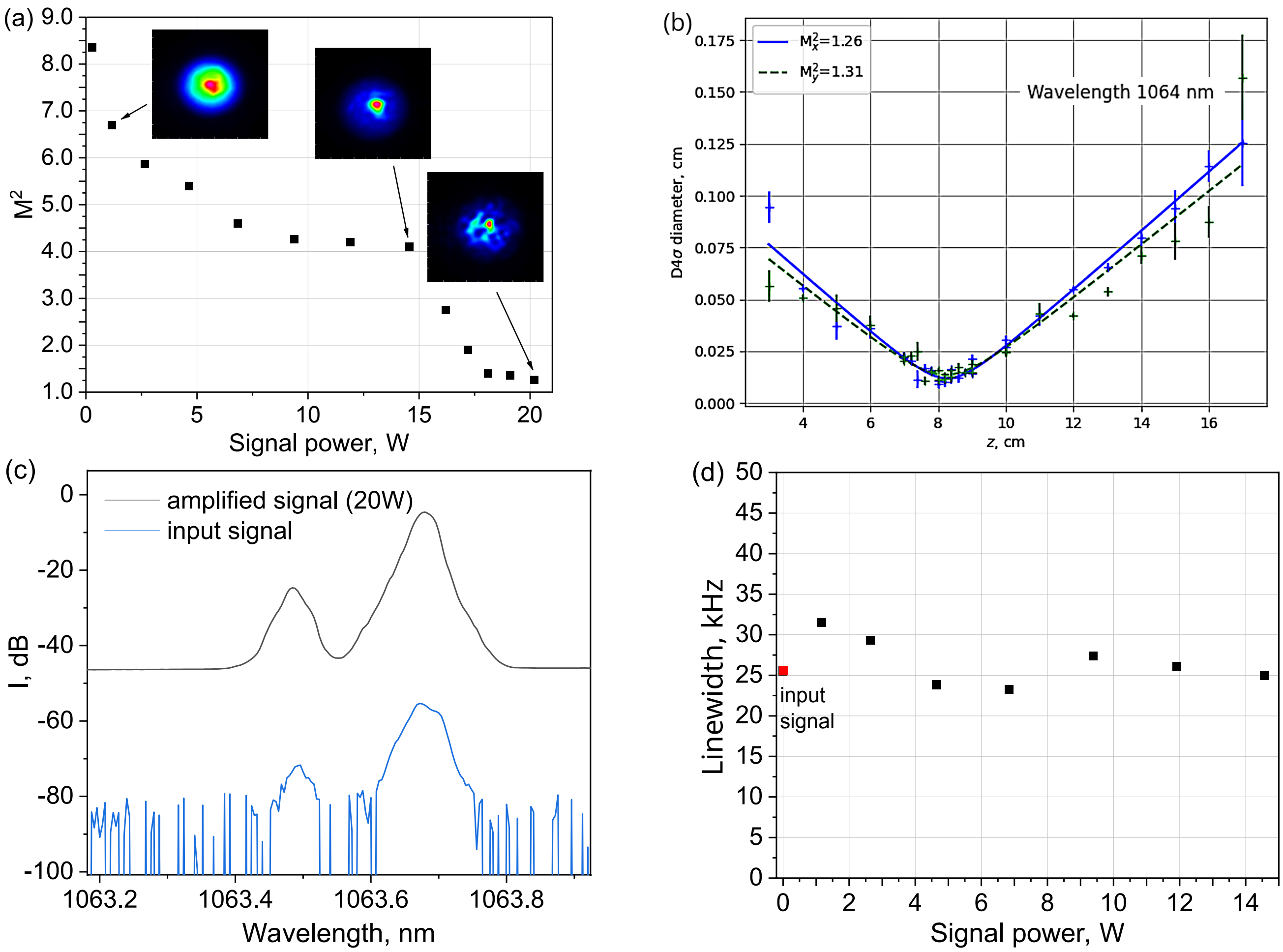

Figure 2. Measured beam quality parameter M^2 as a function of output signal power, which is increased from 0 to ∼15 W by increasing the backward LD pumping, and from ∼15 to ∼20 W by adding forward LD pumping (a); Details of M^2 measurements at the maximum amplifier output power of 20.2 W (b); Signal input and output amplified spectra (c) and signal linewidth measured by heterodyne method as a function of output signal power (d).

As can be seen from Fig. 2(a), our results for the CW output beam quality exhibit a behavior which is analogous what is was reported with sub-nanosecond pulses in a similar taper amplifier with backward pumping.[6] The output beam quality is significantly improved (from the initial $M^2 = 8.4$) with increasing gain until the output power reaches $P_{\text{out}} \sim 10$ W, and it saturates at the level of $M^2 \sim 4$ for further power increases. The details of the M^2 measurements at maximum amplifier output power of 20.2 W are shown in Fig. 2(b). The measured optical spectrum is not changed after amplification (see Fig.2(c)). At the same time, the signal linewidth (as measured by the self-heterodyne method) is kept within its initial value of about 30 kHz (depicted on Fig.2(d)). It should be remarked that in the present case the beam cleaning and its saturation for the amplified CW SF radiation occur at ∼3 orders of magnitude lower signal power (10–15 W) than in Ref.[6] Moreover, when we added a forward LD pumping, the output signal power increases to 20 W, while its beam quality is improved to the level $M^2 < 1.5$, corresponding to a nearly diffraction-limited beam. Although some noisy speckled background is visible at the highest power, the main part is conserved in the bright central spot.

Summarizing, we demonstrated the amplification of a CW SF signal to ∼20 W level in a MM Yb-doped GRIN fiber taper with excellent output beam quality and narrow linewidth, which are comparable with the values

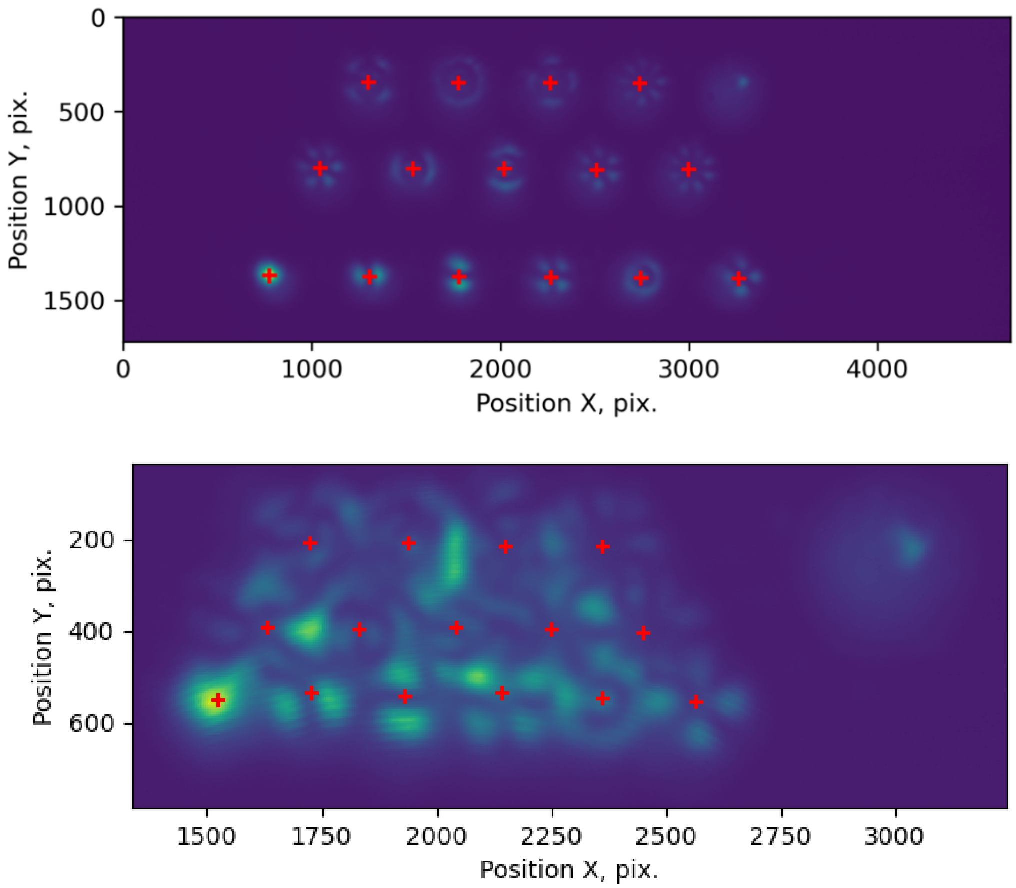

Figure 3. The experimentally captured array of correlation responses for 15 modes. For the lower plot, the characteristic frequency is two times higher than for the case shown in the upper plot. The red crosses indicate the center points of each response, from which the modal amplitudes were retrieved.

obtained with a nearly-singlemode fiber taper,[7] but eliminate its significant drawback – the high sensitivity to fiber bending. To clarify the mechanism of CW SF beam cleaning at such low power levels, we applied a MD technique,[8] and obtained the transverse mode distribution of the output beam as a function of signal power. In additions, we have analyzed the real-time evolution of the mode power distribution.

In order to do this, we used a combination of the phase correlation filter (PCF) method with a matrix-oriented mode decomposition. This unique approach allows us to simultaneously measure the contribution of 15 modes, which is a full set of the first 5 groups of degenerate modes, arranged by their propagation constant. The used setup was the same as in[9] including a spatial light modulator (Meadowlark SLM 1920x1200) and high-speed camera (XIMEA CB160MG-LX-X8G3). The key point here is the calculation of the phase mask, where the phase profiles of the different modes were combined with their individual carrier frequencies. By selecting their values, one can change the distance between the correlation responses (or first diffraction orders of the phase mask) that occur in the far-field after beam modulation by a phase mask. We determined the parameters of the phase masks so that the responses were equidistant from each other. Thus, one of the key parameters in the calculation was the characteristic frequency. By means of our new method, it was possible to measure not only the amplitudes of the modes from the pattern in the far-field, but it was also possible to obtain the intermodal phases in one measurement, thanks to the capability of a matrix-oriented MD.[10] However, one should carefully tune the characteristic frequency for this purposes, since in this case there are two undesirable extremes. On the one hand, when the responses are too close, interference between them begins to affect the intensity at the

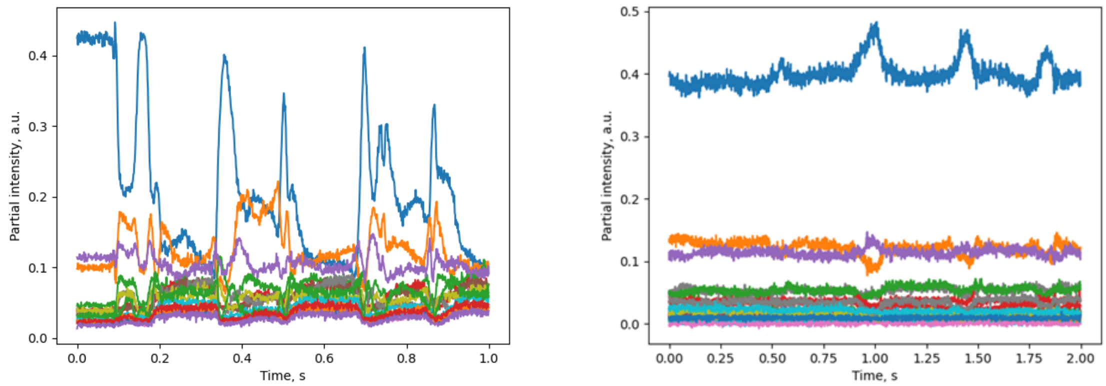

Figure 4. Temporal mode dynamics from the tapered MM GRIN fiber amplifier for different signal output powers (and corresponding counter-propagating pump powers): a) 1.5 W (16 W), b) 14.5 W (50.3 W).

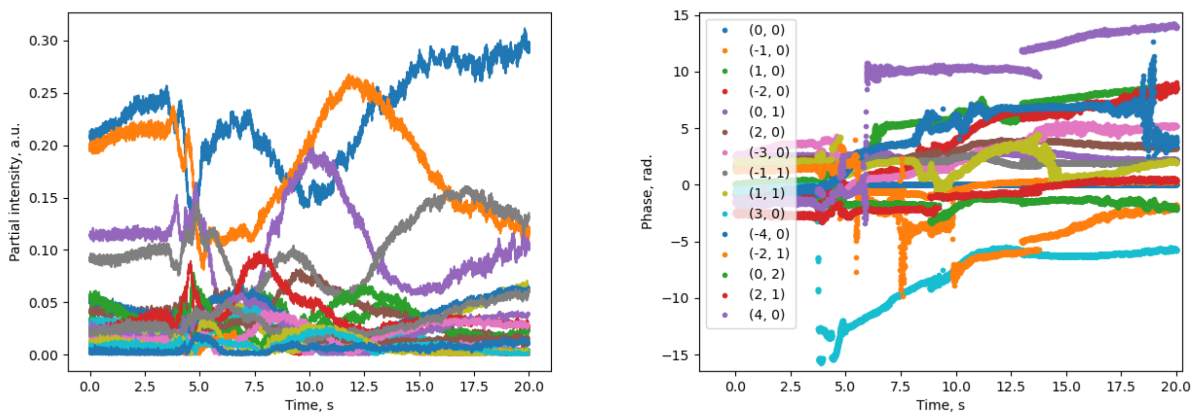

Figure 5. Mode amplitudes (left) and relative phases (right) dynamics in the MM GRIN fiber tapered amplifier during the start of generation obtained with the use of multiplexed PCF method with enhanced post-processing.

center of the correlation response, from where the mode amplitude value is obtained. On the other hand, when the responses are too far apart, the interference is weak, and it becomes impossible to determine the intermodal phases. The experimentally recorded arrays of correlation responses for different values of the characteristic frequency are shown in Fig. 3. Here the red crosses indicate the center points of each response, from which the modal amplitudes were retrieved. These points were obtained during the calibration stage, when the fundamental mode pattern was applied for each correlation response, so that all of them became identical. It should be noted that the additional response (16th in the top right corner) was reserved to observe the far field. In this case, only a constant attenuation was applied without a modal content.

The experimentally measured mode dynamics of the beam are presented in Fig. 4. The stability of the modal content under mechanical tension was checked at both low and high powers. Note that at high output powers the fundamental mode (blue line on Fig. 4) remains much more stable: the amplitude of oscillations drops down to ∼10% from >60% fluctuations in the low power case. This is accompanied by a significant reduction of intermodal energy exchanges, with 40–50% of power kept in the fundamental mode. These observations lead to the conclusion that the beam profile at high powers is more robust, which in turn indirectly indicates the occurrence of beam self-cleaning.

Next we measured the mode dynamics during the amplifier turn-on for the first 20 seconds of operation (see Fig. 5). The data was post-processed with a modified algorithm. As a result, we could obtain the mode amplitudes (Fig. 5a) and phases (Fig. 5b) with a high accuracy. The pump power was increased (by enabling the co-propagating pump) after about 3.5 seconds. This can be revealed by small decrease of the rapid oscillations (due to electrical noise of the detection device), and is accompanied by fast changes of the mode amplitudes and their relative phases. The pump power settled in about 1–1.5 seconds, so that after about 5 seconds it remains stable. Despite that, a slow evolution of both amplitude and phase distributions is observed for about 15 seconds, which could be related to the establishment of a thermal equilibrium inside the taper. At the same time, Fig. 5b) shows that the phase dynamics contains a few jumps at the point in time where the mode with maximum power is interchanged. Such jumps could be related to imperfections of the enhanced MD algorithm, which requires further improvements of the post-processing procedures.

4. CONCLUSION

In conclusion, our study of CW single-frequency signal amplification in a multimode GRIN fiber taper has revealed the presence of a beam cleaning effect which occurs for 3 orders of magnitude lower output power than that in previous experiments with 10 kW sub-nanosecond pulses.[5,6] The output beam was characterized in terms of output power, optical and radio-frequency spectrum, heterodyne-measured linewidth, and beam shape and quality factor (M^2). In the measurements, we initially increased the backward counter-propagating pump power from 0 to 50 W, so that the output signal increases to 15 W. Next, we added pumping from the narrow end of the taper, so that the output signal further grows from 15 to 20 W with the additional forward pumping of 15 W. Backward pumping improves the output beam quality from $M^2 \sim 10$ to ~ 4, whereas adding forward pumping leads to a further beam cleaning to $M^2 < 1.5$. To study the mechanism of the CW SF beam cleaning at such low power levels, we performed a mode decomposition in real-time. This reveals the presence of high-amplitude instabilities (>60%) of the mode amplitudes at low powers. On the other hand, the beam remains relatively stable (∼10%) at high powers. Beam cleaning leads to the fundamental mode power of about 40–50% of the total output power, which limited time-dependent intermodal energy exchange. It may be concluded that the beam profile becomes stable at high powers, with a predominant content of the fundamental mode. In order to fully understand the mechanism of beam-cleaning the in tapered MM amplifier, including the relative role of gain and Kerr nonlinearity, analytical[11] and numerical studies of the beam propagation[12–14] will be necessary.

ACKNOWLEDGMENTS

The authors acknowledge financial support by the Russian Science Foundation (21-72-30024-П) and the European Innovation Council (Grant no. 101185664).

REFERENCES

[1] Richardson, D. J., Fini, J. M., and Nelson, L. E., "Space-division multiplexing in optical fibres," *Nature photonics* **7**(5), 354–362 (2013).

[2] Krupa, K., Tonello, A., Barthélémy, A., Mansuryan, T., Couderc, V., Millot, G., Grelu, P., Modotto, D., Babin, S. A., and Wabnitz, S., "Multimode nonlinear fiber optics, a spatiotemporal avenue," *APL Photonics* **4**(11) (2019).

[3] Wright, L. G., Wu, F. O., Christodoulides, D. N., and Wise, F. W., "Physics of highly multimode nonlinear optical systems," *Nature Physics* **18**(9), 1018–1030 (2022).

[4] Krupa, K., Tonello, A., Shalaby, B. M., Fabert, M., Barthélémy, A., Millot, G., Wabnitz, S., and Couderc, V., "Spatial beam self-cleaning in multimode fibres," *Nature photonics* **11**(4), 237–241 (2017).

[5] Niang, A., Mansuryan, T., Krupa, K., Tonello, A., Fabert, M., Leproux, P., Modotto, D., Egorova, O., Levchenko, A., Lipatov, D. p. S., et al., "Spatial beam self-cleaning and supercontinuum generation with yb-doped multimode graded-index fiber taper based on accelerating self-imaging and dissipative landscape," *Optics express* **27**(17), 24018–24028 (2019).

[6] Niang, A., Modotto, D., Tonello, A., Mangini, F., Minoni, U., Zitelli, M., Fabert, M., Jima, M. A., Egorova, O., Levchenko, A. E., et al., "Spatial beam self-cleaning in tapered yb-doped grin multimode fiber with decelerating nonlinearity," *IEEE Photonics Journal* **12**(2), 1–8 (2020).

[7] Trikshev, A., Kurkov, A., Tsvetkov, V., Filatova, S., Kertulla, J., Filippov, V., Chamorovskiy, Y. K., and Okhotnikov, O. G., "A 160 w single-frequency laser based on an active tapered double-clad fiber amplifier," *Laser Physics Letters* **10**(6), 065101 (2013).

[8] Kharenko, D. S., Revyakin, A. A., Gervaziev, M. D., Ferraro, M., Mangini, F., and Babin, S. A., "Accuracy of holographic real-time mode decomposition methods used for multimode fiber laser emission," in [*Photonics*], **10**(11), 1245, MDPI (2023).

[9] Gervaziev, M., Kuznetsov, A., Revyakin, A., Simonov, V., Dostovalov, A., Terentyev, V., Kharenko, D., and Babin, S., "Real-time mode dynamics of stokes beam in multimode raman fiber laser with mode-selective mirror," *Optics & Laser Technology* **184**, 112512 (2025).

[10] Manuylovich, E. S., Dvoyrin, V. V., and Turitsyn, S. K., "Fast mode decomposition in few-mode fibers," *Nature communications* **11**(1), 5507 (2020).

[11] Agrawal, G. P., "Spatial beam narrowing in multimode graded-index fiber amplifiers: an analytic approach," *Opt. Lett.* **48**, 259–262 (Jan 2023).

[12] Jima, M. A., Tonello, A., Niang, A., Mansuryan, T., Krupa, K., Modotto, D., Cucinotta, A., Couderc, V., and Wabnitz, S., "Numerical analysis of beam self-cleaning in multimode fiber amplifiers," *J. Opt. Soc. Am. B* **39**, 2172–2180 (Aug 2022).

[13] Chen, Y.-H., Haig, H., Wu, Y., Ziegler, Z., and Wise, F., "Accurate modeling of ultrafast nonlinear pulse propagation in multimode gain fiber," *J. Opt. Soc. Am. B* **40**, 2633–2642 (Oct 2023).

[14] Haig, H., Bender, N., Chen, Y.-H., Dhar, A., Choudhury, N., Sen, R., Christodoulides, D. N., and Wise, F., "Gain-induced kerr beam cleaning in a femtosecond fiber amplifier," *J. Opt. Soc. Am. B* **40**, 1510–1517 (Jun 2023).